INORGANIC CHEMISTRY FRONTIERS

RESEARCH ARTICLE

View Article Online
View Journal

Cite this: DOI: 10.1039/d6qi00661b

Cytotoxicity and immunogenic cell death studies of water-soluble tetrahedral Ga(III) or Fe(III) coordination cages containing a Au(I) anticancer drug as guest

Priya Ranjan Sahoo,[a] Fatima Aftab,[b,c] Aaron A. Manu,[b,c,d] Anwita Roy,[a] Maria Contel *[b,c,d,e,f] and Janet R. Morrow *[a]

Water-soluble tetrahedral coordination cages of Ga(III) (**1**) or Fe(III) (**2**) were studied as carriers for FIN and FIN-ester as gold drugs (FIN = triethylphosphine Au(I) complex of 4-mercaptobenzoate or ethyl ester) in solution and in cell culture. Au(I) complexes remained encapsulated inside **1** or **2** at neutral pH even in the presence of serum proteins but were released at mildly acidic pH values (<6.5). The cytotoxicity response of **1** or **2** containing encapsulated FIN was assessed in two different cancer cell lines (human clear cell renal cell carcinoma ccRCC Caki-1 and murine colon carcinoma CT26) as well as normal cells (human fetal lung fibroblasts IMR-90) over a pH range of 7.5–6.2 and compared to the cages alone or gold drug alone. Free gold(I) complexes were the most highly cytotoxic but showed little selectivity for cancer cells compared to normal cells. FIN encapsulated in either Ga(III) or Fe(III) cages displayed a more selective cytotoxic response in cancer cell lines compared to normal cells. At mildly acidic pH, Fe-FIN (**2a**) gave IC_{50} values of 4 μM in CT26 cells compared to 61 μM in IMR-90 cells. Immunogenic cell death studies of FIN in Caki-1 show significant release of DAMPs ATP and HGMB1 and elicitation of prominent CRT translocation at pH 7.2. Under mildly acidic conditions (pH 6.5) there is a significant decrease in DAMPs release, and no translocation of CRT. FIN encapsulated in **1** displays translocation of CRT under these conditions underscoring the potential of water-soluble cages to transport and stabilize gold drugs.

Received 1st April 2026,
Accepted 5th May 2026

DOI: 10.1039/d6qi00661b

rsc.li/frontiers-inorganic

Introduction

Self-assembled coordination cages consist of metal ions and organic linkers that form various polyhedral shapes and have interior cavities for binding to small molecules.[1,2] The host–guest properties of coordination cages make them useful as catalysts that typically function in organic solvents.[3] In contrast, there are more limited examples of water-soluble cages, especially those that are robust under physiological conditions. Robust, water-soluble cages have applications as hosts for delivering a range of drug-like small molecules and inorganic complexes into cells.[4] Coordination cages have recently been studied in animals as carriers for metallodrugs and as imaging agents for MRI or PET.[5–8]

The success of a coordination cage in drug delivery depends on efficient encapsulation and controlled release of the drug to targeted tissue *in vivo* and to organelles within cells. Related nanocarriers that can selectively differentiate cancer cells from healthy cells are under study as promising vehicles for drug delivery.[9,10] An important consideration is the selective liberation of the drug by biological stimuli.[11,12] Among the available biological triggers, pH is an excellent choice of stimulus to release the drug for therapeutic applications. Tumor microenvironment is more acidic[13–17] than healthy tissue, so that certain pH responsive cages may selectively release the drug molecule in the tumor. To date, the most common nanocarriers include liposomes,[18] nanoparticles,[19] cyclodextrins[20] and MOFs.[21] By contrast, only a few coordination cages have been reported to deliver platinum drugs into the cancer cells as shown by Therrien,[6] Lippard[22] or Casini.[23] These studies report on the use of cationic coordination cages to deliver drugs to cancer cells.[24,25] Metallacages

[a]*Department of Chemistry, University at Buffalo, The State University of New York, Amherst, New York 14260, USA. E-mail: jmorrow@buffalo.edu*
[b]*Department of Chemistry & Biochemistry, Brooklyn College, The City University of New York, Brooklyn, NY, 11210, USA*
[c]*Brooklyn College Cancer Center, Brooklyn College, The City University of New York, Brooklyn, NY, 11210, USA*
[d]*Biochemistry PhD Program, The Graduate Center, The City University of New York, New York, NY, 10016, USA*
[e]*Chemistry PhD Program, The Graduate Center, The City University of New York, New York, NY, 10016, USA*
[f]*Biology PhD Programs, The Graduate Center, The City University of New York, New York, NY, 10016, USA. E-mail: mariacontel@brooklyn.cuny.edu*

are also being explored for imaging applications, the delivery of radioactive isotopes, and as platforms for radiotheranostic strategies.[26–28] Recently it has been shown that anionic tetrahedral coordination cages of Fe(III) are effective MRI probes in mice[5,29–31] and solubilize Au(I) drugs in aqueous solutions for *in vivo* studies.[5] Our interest in coordination cages as Au(I) drug carriers motivated the studies presented here.

Au(I) complexes, particularly those with phosphine or N-heterocyclic carbene ligands, are emerging as promising alternatives to platinum-based chemotherapeutics[32,33] due to their ability to induce cell death including immunogenic cell death[34] and to inhibit tumor progression in several types of cancers. Auranofin (AF), originally used for arthritis, is now under investigation for cancer, alongside newer Au(I) compounds showing improved pharmacological profiles.[35] However, many gold-based drugs still face significant limitations including insufficient selectivity, limited aqueous solubility, and short circulation times which hinder their effective use in cancer therapy and clinical translation. Various types of drug carriers are being explored as delivery vehicles for gold-based drugs.[33] Water-soluble, targeted and stimuli-responsive nanocarriers including immunoliposomes[36] and nanopeptides[37,38] have been used successfully for delivering gold compounds to breast and renal cancer cells.

For the development of coordination cages as Au(I) drug carriers, we chose to study anionic tetrahedral cages that were originally developed by Raymond and co-workers.[39] The Ga(III)-based cages host lipophilic Au(I) and Au(III) complexes and have been studied as catalysts (Scheme 1).[40,41] Analogous paramagnetic Fe(III) cages act as MRI probes[31,42] and encapsulate Au(I) drugs for theragnostic studies in mice.[5] Both the Fe(III) and Ga(III) cages solubilize gold metallodrugs and protect them from reacting with nucleophiles such as the cysteine residues of serum proteins. Our group found that the encapsulated complex $[Au(PEt_3)(OH_2)]^+$ was released at the mildly acidic pH values characteristic of tumor environments but reacted with serum albumin over several hours. For further studies, we sought to encapsulate less reactive drugs such as Au(I) complexes of 4-mercaptobenzoic acid (Hmba) in (Au(Hmba)L) with phosphines or N-heterocyclic carbenes. Compounds of the type (Au(Hmba)(PR_3)) have been especially relevant as components of Ti(IV)-based heterometallic complexes with high efficacy in renal cancer mouse models.[43] Moreover, FIN (Scheme 2) which is structurally related to Auranofin suppresses cancer cell migration and invasion, accompanied by decreased levels of pro-metastatic interleukins, MMPs, and TNF-α. It also inhibits the mitochondrial enzyme thioredoxin reductase (TrxR), often overexpressed in apoptosis-resistant tumors, and downregulates FOXC2 and PECAM-1, markers linked to resistance to genotoxic chemotherapy.[44] In addition, FIN has been an outstanding payload to generate antibody drug conjugates efficacious in HER-2 positive breast cancer mouse models.[45] As part of our endeavour towards understanding Au(I) drug encapsulation and delivery using coordination cages, anionic tetrahedral cages (Scheme 2) including Ga-FIN (**1a**), Ga-EthylFIN (**1b**) and Fe-FIN (**2a**) were studied with a focus on drug release, cytotoxicity and cellular uptake. The cancer cell lines examined in this study

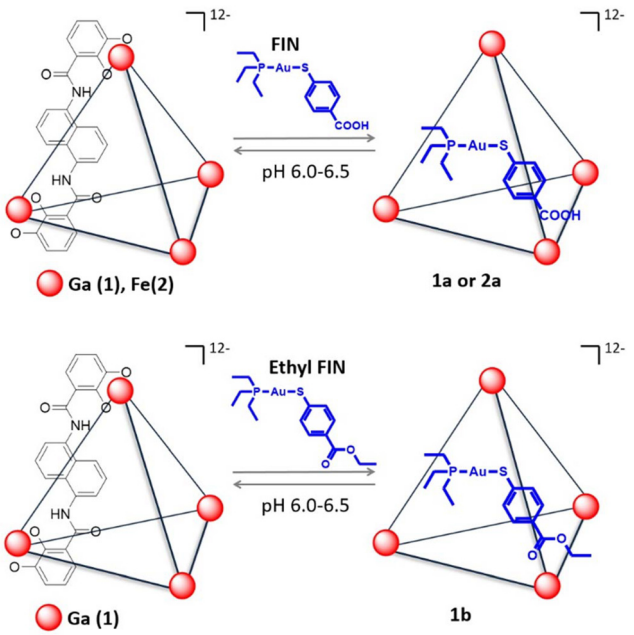

Scheme 2 Encapsulation of FIN or ethyl-FIN complexes within gallium (**1**) or iron (**2**) cage and their release at acidic pH. Linker structure is shown in Scheme S1.

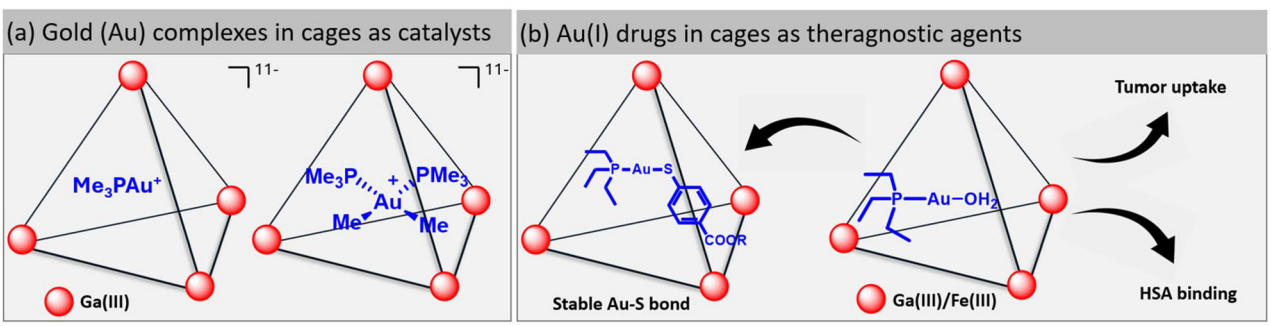

Scheme 1 Illustrations showing Au(I) and Au(III) complexes in coordination cages studied as catalysts (a) or as theragnostic agents (b).

are clear cell renal cell carcinoma (ccRCC) Caki-1 and colon carcinoma CT26. They were selected based on the pronounced activity of FIN [Au(mba)(PEt_3)] and its derivatives in ccRCC across both *in vitro* and *in vivo* models, supported by mechanistic insights.[35,36] Encapsulation of the more labile gold(I) complex Au(PEt_3)Cl within an Fe(III) cage (**2**) resulted in enhanced vascular contrast and increased accumulation in colorectal CT26 tumors in BALB/c mice, as demonstrated by MRI, and enabled intravenous administration, validating Fe and Ga cages as delivery vehicles in colon carcinoma.[5]

Results and discussion

Synthesis and characterization of host–guest complexes

Addition of one equivalent of FIN complex to the Ga(III) cage **1** in D_2O (pD = 8.6) produced a complex showing ^{1}H NMR resonances at −0.26 and −1.7 ppm assigned to the ethyl groups of the phosphine ligands of FIN encapsulated within the cage (Ga-FIN (**1a**)) (Scheme 2 and Fig. 1). The aromatic protons of the FIN complex, which is insoluble in water, shifted from 7.8 and 7.6 ppm in $CDCl_3$ to 6.0 and 5.7 ppm in D_2O following FIN incorporation into the cage. The complicated aromatic ^{1}H NMR resonance pattern of the cage is likely the result of distortion of the tetrahedral cage upon guest incorporation, given that a simple aromatic pattern is restored upon ejection of FIN. The encapsulation of the FIN complex in **1a** is verified by ^{1}H DOSY NMR as shown by the diffusion coefficient (D = 1.44 × 10^{-10} m^2 s^{-1}) determined for all the proton resonances of the host–guest species (Fig. 2). Incorporation of Au(I) complex did not substantially alter the diffusion coefficients in comparison to the native Ga(III) cage (D = 1.77 × 10^{-10} m^2 s^{-1}) in D_2O. Calculation shows a comparable cage radius for Ga(III) cage (1.12 nm) and Ga-FIN cage (1.38 nm). The Fe(III) cage with encapsulated FIN (**2a**) was prepared in a similar manner. Quantitation of the amount of Au *versus* Ga or Fe, as measured by ICP-MS, supported complete encapsulation of gold complexes in the cages when they were precipitated from solution and isolated as solids.

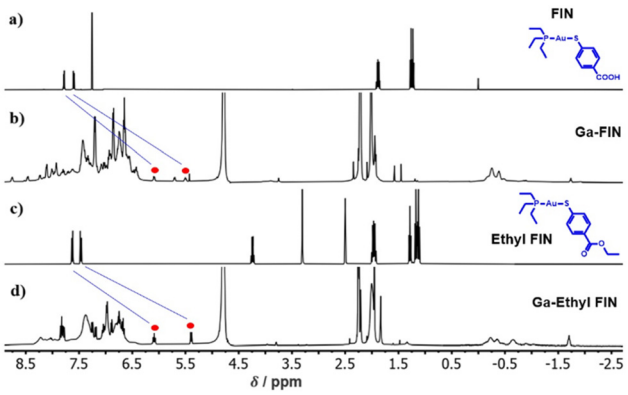

Fig. 1 ^{1}H NMR spectra (400 MHz) of (a) free FIN complex in $CDCl_3$; (b) FIN encapsulated Ga cage in D_2O (Ga-FIN **1a**); (c) FIN-ester complex in DMSO-D_6; (d) FIN-ester encapsulated Ga cage (Ga-ethyl FIN **1b**) in D_2O at pH 7.7. Red circles denote the aromatic proton resonance of the encapsulated gold complexes.

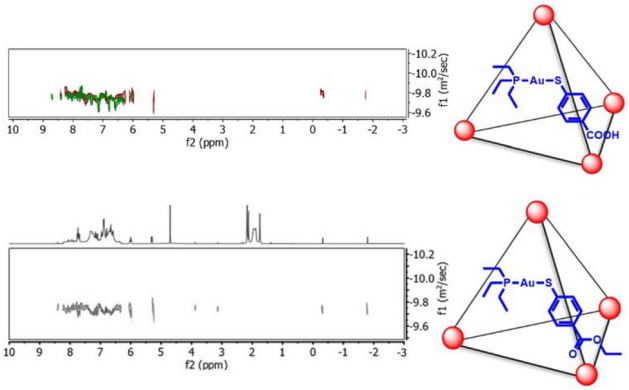

Fig. 2 (Top) Overlay of DOSY spectra (400 MHz) of **1a** (Ga-FIN) shown in orange color, free cage in green color and (bottom) DOSY spectra of **1b** (Ga-ethyl FIN) shown in grey color in D_2O.

The encapsulation of the more lipophilic ethyl ester of FIN was studied for comparison to the FIN complex which is anionic if ionized at the carboxylic acid or neutral if protonated. The spectral characterisation of ethyl-FIN complex is shown in Fig. S1–S5. Given the propensity of the highly anionic coordination cages to encapsulate cationic or neutral guests, we surmise that FIN is most likely in a neutral form in the cage. Moreover, these coordination cages feature an acidic environment that would also favor protonation of the carboxylic group of the FIN guest.[46,47] As shown, the highly shifted ^{1}H NMR peaks at −0.23, −0.64 and −1.71 ppm confirmed encapsulation of neutral ethyl-FIN to generate Ga-EthylFIN (**1b** in Fig. 1). The aromatic proton resonances at 7.6 to 7.4 ppm shifted to 6.0 and 5.4 ppm respectively indicating full encapsulation of the thiol portion of the gold guest. The methylene group of the ethyl ester of ethyl FIN shifted from 4.2 ppm to 3.8 ppm following encapsulation. An increase in diffusion coefficient with D = 1.59 × 10^{-10} m^2 s^{-1} was noted for ethyl-FIN encapsulated in the cage. Similar guests with aromatic groups such as benzyl phosphonium have been studied by Raymond and co-workers within **1**.[48] The ^{31}P spectra of **1a** and **1b** were unchanged for up to 2 weeks in either water or phosphate buffer at pH 7.4 (Fig. S7 and S8). Further, ^{1}H NMR spectra of **1a** in D_2O with dissolved RPMI 1640 cell media (10% FBS) displayed upfield-shifted proton resonances characteristic of the encapsulated triethyl phosphine group as well as aromatic resonances at 5.35–6.0 ppm observed for encapsulated FIN complex (Fig. S9).

Studies of gold drug release and cage stability as function of pH

Prior to cell culture studies, the cages and their encapsulated gold complexes, **1a**, **1b**, **2a** were monitored at various conditions relevant to *in vitro* and *in vivo* environments. Release of gold drug was examined as a function of pH and the robustness of the cages under acidic conditions and with biological reductants were studied. Moreover, it was of interest to identify the gold

species released from the cage given that reactions of compounds within these tetrahedral cages are well-known.[4,5,49]

The effect of pH/pD on gold(I) complex release was studied by ^{1}H NMR spectroscopy. At pD = 6.2, the NMR spectrum of **1a** showed two new ^{1}H resonances at 0.92 ppm and 1.33 ppm corresponding to the released gold(I) complex (Fig. S10) and the original resonances of the encapsulated complex disappeared. The DOSY spectra (Fig. S11) were consistent with the presence of free cage and released Au(I) complex. Release of the encapsulated complex was also supported by ^{31}P NMR studies of **1a** at pD = 6.2 (Fig. S13).[44] Similarly, ^{1}H NMR spectra of **1b** recorded at pD = 6.2 showed resonances corresponding to the released gold complex (Fig. S12) and ^{1}H DOSY spectra of **1b** under these conditions supported the release of ethyl-FIN (Fig. S14). Notably, the mildly acidic conditions of release were similar to that observed in our previous studies of a $[Au(PEt_3)(OH_2)]^+$ as a guest encapsulated in **1**.[5]

Electrospray ionization mass spectrometry (ESI-MS) was used to monitor gold complex ejection and potential change in speciation upon release from Ga(III) and Fe(III) cages as the pH was varied from 8.0 to 5.5. The ejected gold complexes were compared as relative signal intensities by using Bu_4NPF_6 as an internal standard. A major peak at 469.1 was observed at pH 6.5 that was assigned to released FIN complex. However, at more acidic pH values of 6.0 or 5.5, there was a mixture of FIN complex and $[(PEt_3)_2Au]^+$. Similar release profiles were obtained at pH 6.5 for both Ga(III) and Fe(III) cages with peaks corresponding to $[Au(PEt_3)_2]^+$ and to FIN complex (Fig. S15 and S16). Additional experiments were carried out to determine whether the bis-phosphine gold complex was formed inside of the cage or formed from released FIN at acidic pH values. NMR spectra of $[Au(PEt_3)_2]^+$ encapsulated within **1** (Fig. S17 and S18) show proton resonances for the ethyl groups of the phosphine, observed at −0.5 and −1.5 ppm, that are distinct from those of encapsulated FIN (**1a**). This data is most consistent with formation of the gold(I) bis-phosphine complex upon release from the cage at acidic conditions.

The stability of the cages at acidic pH and with physiological amounts of ascorbate was studied towards the elucidation of the mechanism of guest release. Titration of the Ga(III) cage (**1**) from pH 7.4 to pH 4.0 showed no change in the electronic absorption spectrum of the cage over this pH range (Fig. S19), suggesting that the protonation state of the catechol ligands does not change over this pH range. DOSY spectra at pD of 5 showed a similar diffusion constant as that observed at pD 7 (Fig. S11), consistent with the cage remaining intact under acidic conditions. Similar DOSY spectra were observed for solutions of Ga-EthylFIN (**1b**) at pD 6.2 (Fig. S14) with data supporting gold complex dissociation from the cage. By contrast, the Fe(III) cage (**2**) showed a shift in the MLCT band upon titration from pH 8 to pH of 5, indicative of protonation of one or more of the catechol groups (Fig. S19) and fitting of the data gives a pK_a value of 5.8 for protonation of **2**. Adjustment of the pH back to neutral gives the original spectrum, suggesting that the protonation of the catechol group does not destroy the Fe(III) cage structure. The gallium and iron cages were also treated with ascorbate (5–100 μM) as a biologically relevant reductant in the blood pool to gauge the likelihood of reduction of the cage itself.[50] These studies showed that the coordination cages resisted reduction in the presence of ascorbic acid when incubated at 37 °C for 1 hour (Fig. S20). This data is consistent with the highly negative redox potential of tris-catechol Fe(III) complexes[51] which correlates to the stabilization of the trivalent iron center. Moreover, the ^{31}P NMR spectrum of Ga-FIN cage, (**1a**), showed little change suggesting the absence of reaction to ascorbate over 1 hour (Fig. S21).

Cytotoxicity studies

Cytotoxicity data was collected for cages and gold drugs as a function of pH in human clear cell renal cell carcinoma (Caki-1) and murine colon carcinoma (CT26) cells and compared to that in human fetal lung fibroblasts (IMR-90) cells by using the Presto-Blue assay (Table 1 and Tables S1–S5). Data was collected for free cages **1** and **2** and for free Auranofin and for FIN. The Fe(III) and Ga(III) cages alone displayed very moderate antiproliferative effects in all three cell lines (IC_{50} ranging from 40 to 90 μM) with cytotoxicity increasing slightly over the pH range of 7.5 to 6.2, especially in the cancer cell lines (IC50s 48 to 79 μM after 24 h incubation). In comparison, cages with encapsulated FIN (**1a** and **2a**) produced higher cytotoxicity than the free cages and showed selectivity towards cancer cells, especially at pH 6.2 com-

Table 1 Mean IC_{50} values ± SD (μM) on (top) CT26 cells and (bottom) Caki-1 cells after 24 h incubation from three independent experiments. Cages (**1** and **2**) and metal-containing cages (**1a** and **2a**) were dissolved in H_2O and Auranofin and Fin in DMSO (0.1%). Dilutions were performed in media

pH level	Ga-cage (μM)	Fe-cage (μM)	Ga-FIN cage (μM)	Fe-FIN cage (μM)	Auranofin (μM)	FIN (μM)
7.5	63.64 ± 1.34	71.03 ± 1.20	22.66 ± 1.50	29.71 ± 1.46	8.81 ± 0.73	9.31 ± 1.27
7.2	57.15 ± 1.97	65.60 ± 2.43	17.84 ± 1.34	22.53 ± 1.03	5.99 ± 0.40	7.20 ± 0.54
6.5	50.07 ± 2.31	59.05 ± 3.20	8.32 ± 0.99	10.28 ± 2.33	3.79 ± 0.40	5.58 ± 0.47
6.2	48.24 ± 3.51	53.01 ± 2.36	4.78 ± 0.35	5.50 ± 0.40	3.28 ± 0.65	4.13 ± 0.25
pH level	Ga-cage (**1**)	Fe-cage (**2**)	Ga-FIN cage (**1a**)	Fe-FIN cage (**2a**)	Auranofin	FIN
7.5	65.97 ± 1.27	79.38 ± 1.59	23.92 ± 1.03	31.37 ± 1.19	7.35 ± 0.59	8.82 ± 0.87
7.2	59.76 ± 1.35	70.15 ± 1.87	18.87 ± 0.92	23.34 ± 0.71	5.33 ± 0.33	6.60 ± 0.44
6.5	53.32 ± 1.87	65.61 ± 2.17	10.33 ± 0.67	12.78 ± 1.88	4.71 ± 0.32	5.94 ± 0.38
6.2	50.02 ± 2.41	58.11 ± 1.90	5.93 ± 0.28	6.81 ± 0.33	3.46 ± 0.51	4.12 ± 0.17

pared to physiological pH. After a 24 h treatment, the Ga(III) and Fe(III) cages containing the gold guest exerted good potency against Caki-1 (IC_{50} = 5.93 ± 0.28 μM for Ga-FIN **1a**, and 6.81 ± 0.33 μM for Fe-FIN **2a)** and CT26 cells (IC_{50} = and 4.78 ± 0.35 μM, for Ga-FIN **1a** and 5.50 ± 0.40 μM for Fe-FIN **2a**) at pH 6.2 (Table 1 and Fig. 3). The potency of complexes improved slightly after 72 h of incubation at pH 6.2. Under these conditions, IC_{50} values of 3.86 ± 0.11 μM and 4.43 ± 0.35 μM in Caki-1 cells and IC_{50} values of 3.28 ± 0.24 μM and 3.77 ± 0.28 μM in CT26 cells were observed for **1a** and **2a**, (Tables S1–S5). The improved antiproliferative effect at acidic pH was observed in the cancer cell lines (Fig. 3 and 4), but much less so in the non-malignant lung fibroblast cells (Fig. 3 and S22). The free gold complexes, Auranofin and FIN showed very little selectivity for the cancer cell lines compared to normal cell lines with all IC_{50} values decreasing slightly with pH for the free gold drugs.

^{69}Ga and ^{197}Au quantification in cell lysates (ICP-MS)

Studies were carried out in murine colorectal cancer (CT26) cells to assess cellular uptake of FIN as a free drug or when encapsulated in the Ga(III) cage (**1**) or Fe(III) cage (**2**). Quantification of Au, or Ga was studied by using ICP-MS analysis upon digestion of the cells or organelles in concentrated acid. Analysis of experiments with **2a** were analyzed for Au but not Fe uptake due to the presence of native iron in the cells that would interfere with measurements.

Studies with the Fe(III) cages as carriers show that total Au cellular content is similar with free drug and with encapsulated FIN (**2a**) (Fig. 5 & S27). Studies with the Ga(III) cage as a carrier had the advantage that the cage itself could be tracked and showed that Au was taken up into the cells both as free drug and when encapsulated in **1**. Surprisingly, the Ga content found in whole cells for experiments using the cage alone or as Ga-FIN (**1a**) was substantial. A possible explanation is that

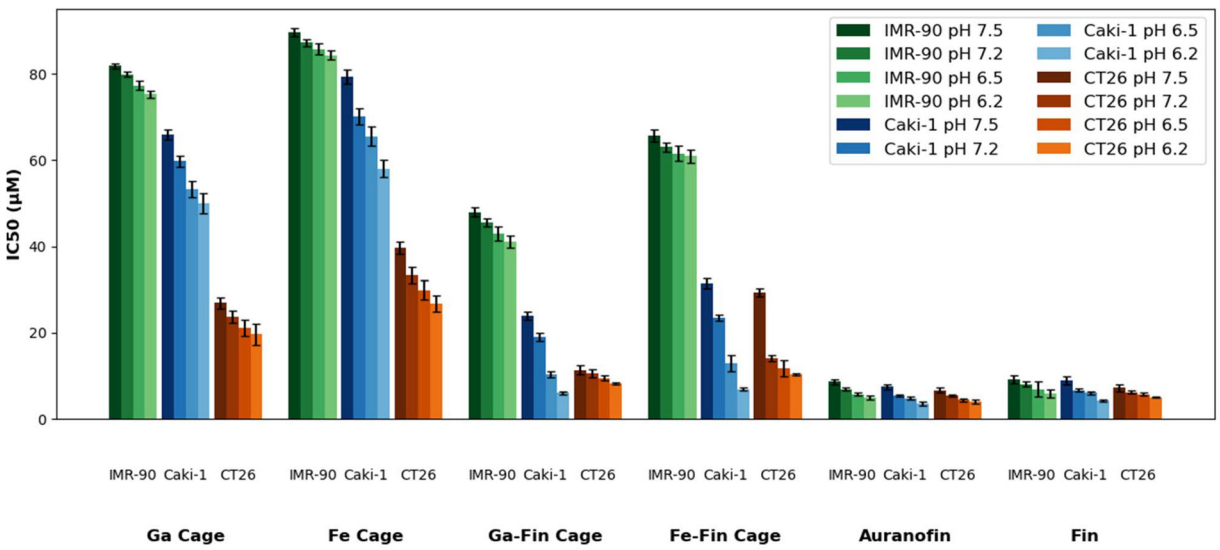

Fig. 3 Bar diagram showing the IC_{50} values for native cages, cages with encapsulated Au(I) drugs, and free gold complex FIN against IMR-90, Caki-1 and CT26 at four different pH values after 24 h incubation. Auranofin was used for comparison purposes.

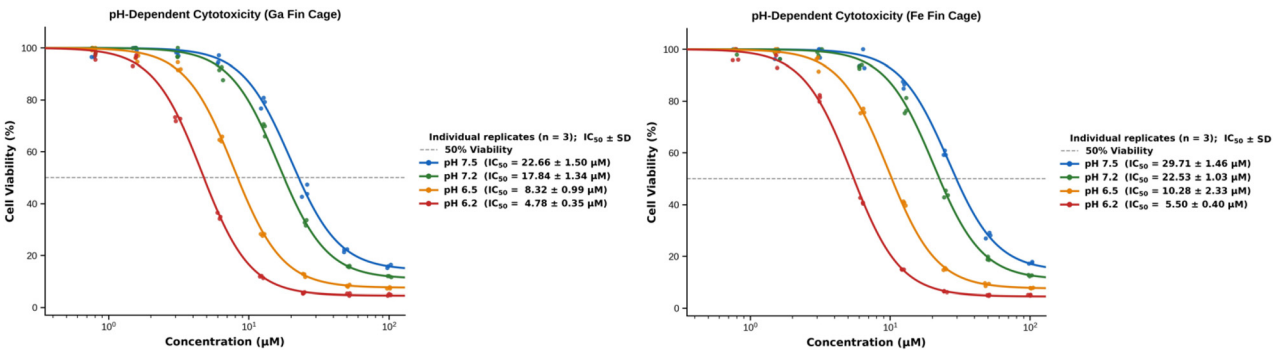

Fig. 4 pH-dependent cell viability profile of (left) Ga-FIN (**1a**) and (right) Fe-FIN (**2a**) cages on CT26 cells at different concentrations (Presto-Blue assay). Curves were fitted using four-parameter logistic (4PL) regression. Individual data points from three independent experiments (n = 3) are shown. IC_{50} values ± SD are reported in the legend; the dashed line indicates 50% viability.

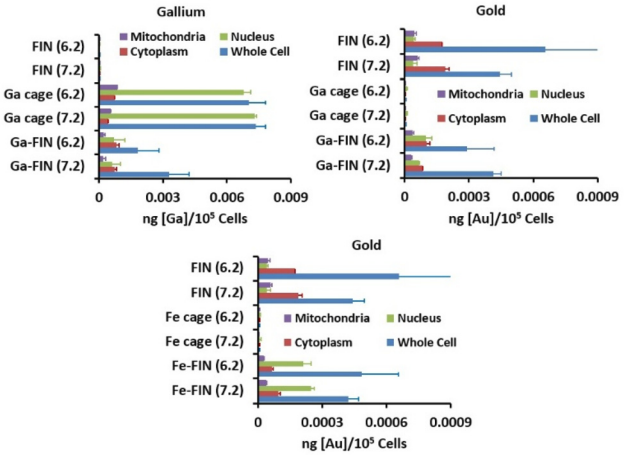

Fig. 5 Cellular internalization of Ga and Au from **1a (Ga-FIN)**, **2a (Fe-FIN)**, native Ga cage (**1**) in whole CT26 cells, cytoplasm, nucleus and mitochondria at pH 7.2 and 6.2 as measured by ICP-MS. The respective pH values are given in parentheses.

binding of the cage to human serum albumin may facilitate cellular uptake. Our previous studies showed that both **1** and **2** bind strongly to serum albumin.[31,42] The nearly 4 : 1 ratio of Ga to Au in whole cells is consistent with **1a** being taken up into the cells as a unit or with similar uptake of cage and FIN separately (Fig. 5).

Sub-cellular fractionation was carried out to analyse the organelles for Au content. Notably, cytoplasmic Au content was about two-fold higher for free drug than with either **1** or **2** as a carrier (Fig. 5, S27 and S28). Very little gold was measured in the mitochondria with or without the Ga(III) or Fe(III) cages as carriers. However, gold content increased in the nucleus with both **1** and **2** cages as carriers. This corresponds to the large amount of Ga found in the cell nucleus and suggests that gold is transported into the nucleus by the cage. Differences in uptake at pH 7.2 and 6.2 over 24 hours were minimal for these two pH values.

Immunogenic cell death studies

Immunogenic cell death (ICD) is a form of regulated cancer cell death that elicits an adaptive immune response against tumor cells. This phenomenon is defined by the emission of damage-associated molecular patterns (DAMPs), notably the extracellular release of adenosine triphosphate (ATP), secretion of high mobility group box 1 protein (HMGB1), and the translocation of calreticulin (CRT) to the plasma membrane. These immunostimulatory signals facilitate dendritic cell recruitment and maturation, enhance antigen uptake and processing, and promote the activation of tumor-specific T lymphocytes, thereby coupling direct tumor cell killing with the establishment of immunological memory.[52,53] Notwithstanding its therapeutic relevance, the repertoire of clinically validated ICD-inducing agents remains narrow. Only a small subset of FDA-approved chemotherapeutics including anthracyclines (doxorubicin, mitoxantrone), platinum agents (oxaliplatin), and others (such as Lurbinectedin, Bortezomib, and Cyclophosphamide) have been shown to reliably trigger ICD.[52–55] However, their clinical performance is frequently limited by the emergence of drug resistance, dose-limiting toxicities, and insufficient tumor selectivity.[56] These limitations underscore the need to develop next-generation ICD inducers that operate through alternative molecular pathways and retain efficacy in recalcitrant malignancies such as clear cell renal cell carcinoma (ccRCC).

Gold compounds are emerging as potential ICD inducers,[34,57–65] but no studies have been reported for metal-based anticancer agents encapsulated in nanocarriers. Immunogenic cell death in clear cell renal carcinoma remains largely underexplored, yet it holds significant potential for informing the development of novel therapeutic strategies.[66] Mitoxantrone in combination with cholesteryl indoximod in a liposomal combination has been found to have a limited effect in tumor growth in a renal cancer syngeneic model (RENCA)

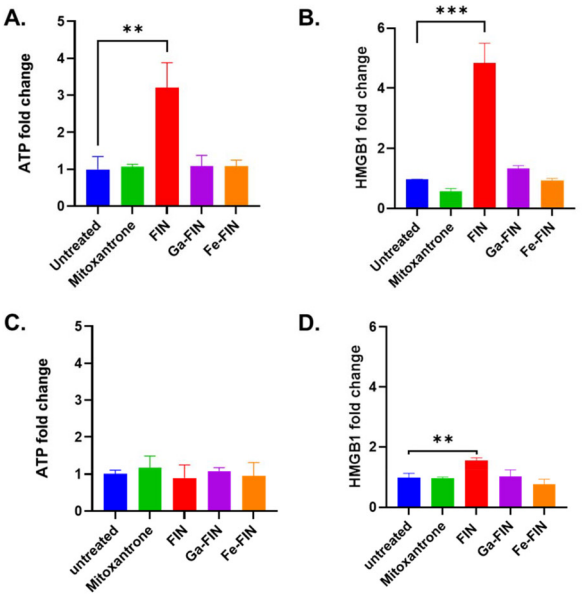

Compounds	IC_{50} at pH 6.5 (μM) 24h	IC_{50} at pH 7.2 (μM) 24h
Mitoxantrone	1.84 ± 0.37	4.17 ± 0.38
FIN	5.94 ± 0.38	7.7 ± 0.28
Ga-FIN	10.33 ± 0.67	18.87 ± 0.92
Fe-FIN	12.78 ± 1.88	23.34 ± 0.71

Fig. 6 Extracellular release of ATP and HMGB1 using IC_{50} concentrations of compounds and 24 h incubation. (A) Release of ATP at pH = 7.2; (B) release of HGMB1 at pH = 7.2; (C) release of ATP at pH = 6.5; (D) release of HGMB1 at pH = 6.5. Data represents SD from n = 3 independent biological replicates. Statistical analysis was performed using unpaired student t-test and a p value <0.05 is considered statistically significant. **p < 0.0021, ***p < 0.0002.

despite the efficient release of DAMPs and CRT translocation of Mitoxantrone.[67] Promising results (tumor volume decrease and lack of systemic toxicity) in ccRCC mice models with heterometallic compounds containing molecules like FIN encouraged us to explore the ICD potential of FIN free and encapsulated in the Ga(III) and Fe(III) cages. Here we evaluate the release of extracellular ATP and HGMB1 as well as the translocation of CRT in ccRCC caki-1 cells treated with IC_{50} concentrations of FIN, Ga-Fin and Fe-Fin for 24 h. We carried out the incubation at pH = 7.2 and pH = 6.5 and evaluated mitoxantrone as a positive control for ICD. The results of the release of extracellular ATP and HMGB1 for the two pH values are collected in Fig. 6.

Extracellular ATP release was quantified in Caki-1 clear cell renal carcinoma (ccRCC) cells following 24 hour treatment with FIN, Ga-FIN, and Fe-FIN complexes at their respective IC_{50} concentrations under two conditions, acidic (pH 6.5) and physiological (pH 7.2). Supernatants were collected, and ATP levels were measured using a luciferase-based luminescence assay. FIN and positive control Mitoxantrone induced the highest levels of ATP release among the tested compounds, while Ga-FIN (**1a**) and Fe-FIN (**2a**) cages did not trigger detectable ATP secretion above baseline levels at pH 7.5 (Fig. 6a). HMGB1 release was evaluated using an ELISA assay to measure its release from the nucleus to the extracellular medium in Caki-1 cells. Treatment with FIN led to the higher HMGB1 release, while mitoxantrone, Ga-FIN (**1a**) and Fe-FIN (**2a**) did not show release relative to untreated controls (Fig. 6b).

The cages release gold compounds at lower pH, so these experiments were also performed at pH = 6.5. At this slightly acidic pH, the release of ATP and HGMB1 decreases considerably for FIN and there is not much variation for mitoxantrone, the Ga-FIN and Fe-FIN cages. Mitoxantrone is known to be less cytotoxic at lower pH as it dimerizes, inhibiting cellular uptake and resulting in accumulation of cells in G, phase in breast and bladder, where they may be more resistant to mitoxantrone and related molecules.[68,69] However these effects are dose dependent. In caki-1 we see an increase in cytotoxic potential and no changes while decreasing the pH from 7.2 to 6.5. For FIN the cytotoxicity also increases slightly while decreasing the pH, but the release of DAMPs decreases significantly. To elucidate these results, NMR experiments were carried out to study the speciation of FIN under mildly acidic conditions. Upon decreasing the pD value from 7.2 to 6.5, minor resonances appear in the aromatic region of the NMR spectrum (Fig. S29). These are likely due to dissociation of the thiol ligand and subsequent formation of $[Au(PEt_3)_2]^+$. This was also corroborated with ^{31}P NMR where a new resonance appears at 47.1 ppm amounting to 15% along with the original major peak at 38.1 ppm assigned to the bis-phosphine complex and FIN complex respectively (Fig. S30). However, most of the FIN complex remains intact under these conditions, suggesting that other factors are important in the ICD response.

Calreticulin (CRT) is predominantly endoplasmic reticulum-localized but undergoes membrane translocation during ICD, resulting in surface exposure as ecto-CRT.[70] CRT translo-

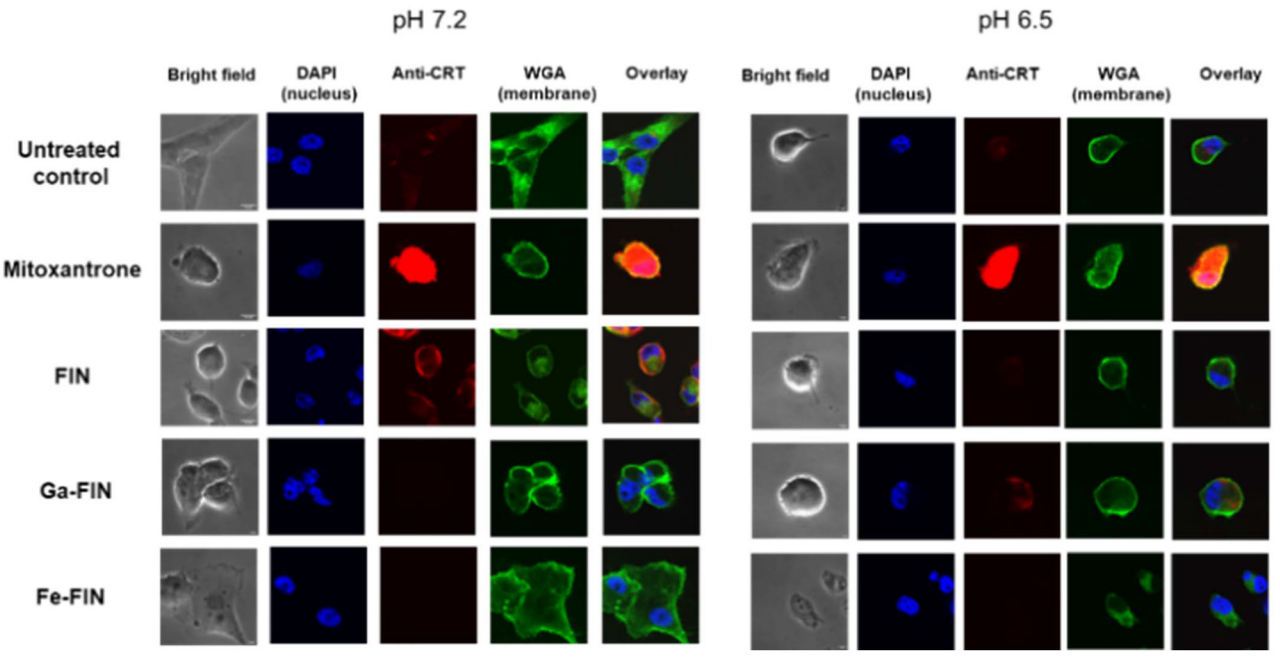

Fig. 7 Representative immunofluorescence images showing ecto-calreticulin (CRT) exposure in Caki-1 cells after 24 hour treatment with the specific compounds at their respective IC_{50} concentrations under neutral (pH 7.2) and mildly acidic conditions (pH 6.5). Cells were stained with anti-CRT antibody (detect surface-exposed CRT), wheat germ agglutinin (WGA) staining the plasma membrane, and DAPI to stain the nuclei. n = 2–3 independent replicates. Images were acquired by confocal microscopy using identical acquisition settings across all conditions. Scale bar is 10 μm.

cation to the cell surface is one of the main hallmarks of immunogenic cell death (ICD), functioning as an "eat-me" signal that promotes dendritic cell phagocytosis of dying tumor cells. To evaluate this response, Caki-1 renal cancer cells were treated with the selected Au(I) compounds at their respective IC_{50} concentrations for 24 hours. Following treatment, cells were stained with anti-CRT antibody and analyzed *via* fluorescence microscopy (Fig. 7) as reported by Babak and coworkers in MPM tumors.[34] At pH = 7.2, FIN treatment resulted in prominent CRT exposure at the plasma membrane, as evidenced by co-localization of CRT signal with WGA staining. In contrast, Ga-FIN (**1a**) and Fe-FIN (**2a**) cages did not induce detectable CRT translocation. Untreated cells exhibited minimal CRT exposure.

As described for other ccRCC cells, the positive control mitoxantrone induced high CRT exposure. At pH 6.5, FIN treatment did not result in noticeable CRT exposure to the plasma membrane. However, when encapsulated in the Ga cage (**1a**) showed slight exposure of CRT. Fe-FIN (**2a**) cages did not induce detectable CRT translocation. Further studies will address more time points and pH, to find the optimal translocation conditions. It is important to note that in epithelial cancer cell lines such as Caki-1 (human clear cell renal carcinoma), exposure to cytotoxic agents or targeted therapies can lead to the disruption of the cell cycle, which can cause cells to lose their ability to adhere to the culture surface. Cell rounding is a sign of stress, and cell detachment or changes in cell shape indicate dying cells or cells in a resistant state (as observed for cells treated with the compounds, Fig. 7).[71,72] In addition, extracellular pH is a critical factor in cellular processes. This directly affects metabolic activity, enzymatic function, and cytoskeleton polymerization.[73] Generally, the optimal pH range of 7.2 to 7.4 is required for normal, healthy morphology. Variations lead to stress, causing cells to round up, shrink or detach from the surface of the flask. These effects can be observed for some of the treated cells.

Collectively, these results indicate that, while FIN is a potent inducer of immunogenic cell death at pH 7.2, at mildly acidic pH its ICD properties significantly decrease (especially CRT translocation). Encapsulation in cages (as shown by Ga-FIN **1a**) may preserve its ICD potential.

Conclusions

Two Au(I) triethyl phosphine complexes (FIN and ethyl-FIN) containing aryl thiolate ligands were studied here as guests within tetrahedral Ga(III) or Fe(III) cages. FIN and related [Au(mba)L] (L = PR_3, NHC) compounds are of interest as components of Ti–Au anticancer drugs and antibody drug conjugates in cell culture and in animal tumor models.[38,45] Moreover, FIN has displayed relevant anticancer properties as a free compound.[44] Solution studies of **1a**, **2a** and **1b** suggest that the FIN or EthylFIN complexes are released at slightly acidic pH values. Previously, we showed that a related gold complex was also released at weakly acidic pH values.[5] The similarity of the pH of release for the three complexes suggests that the aqueous interior of the cage is altered as the external pH is changed, and that this cavity environment is less favourable to Au(I) complex encapsulation. For the Fe(III) cage, protonation of the catechol groups may play a role in the change of environment, but the Ga(III) cage shows no such change in protonation state.

The host–guest complexes of the cages with Au(I) drugs discussed here have excellent water solubility (millimolar) and are compatible for studies in cell culture as drug carriers. Whereas the free gold complexes, Auranofin and FIN, were highly cytotoxic, there was little selectivity for cancer cells compared to normal cells. In comparison, the cages alone showed little cytotoxicity towards either normal or cancer cells. The cages **1** and **2** with encapsulated FIN showed an intermediate toxicity towards the two cancer cell lines at neutral pH and maintained selective toxicity towards cancer cells. Cytotoxicity increased as pH was lowered for Au(I) complex alone, cage alone and for the host–guest complexes of cage with encapsulated FIN. However, the effect was most pronounced for the encapsulated FIN complexes (**1a** and **2a**). At a pH of 6.2, the FIN complex encapsulated in the Fe(III) cage or in the Ga(III) cage showed IC_{50} values of 3–4 μM towards the cancer cell lines. Importantly, the Fe(III) cage or Ga(III) cage with encapsulated FIN gave the same potent cytotoxicity at pH 6.2 as did free FIN, but with a much higher selectivity for killing cancer cells. The greater cytotoxicity at acidic pH may be attributed to greater release of the gold complex from the cage. Our studies also demonstrated that while FIN displays relevant immunogenic cell death properties at pH 7.2 in ccRCC caki-1 cells, at a mildly acidic pH (6.5) the release of DAMPs and translocation of CRT are diminished. However, when encapsulated in the Ga(III) cage (**1a**) at this pH, there is still translocation of CRT, indicating that these water-soluble cages can indeed serve as useful delivery carriers for anticancer gold(I) drugs.

The tetrahedral Fe(III) cages are of interest as MRI probes that accumulate in murine tumor models over a 1 to 24 hours period and function as hosts for metallodrugs.[5] The role of the coordination cage was to carry the metallodrug to the tumor site and release the drug under the acidic pH values in tumor tissue. However, studies here show that the Ga(III) cage, as an isostructural model for the Fe(III) cage, is taken up into cancer cells over a 24 hour period. If the Fe(III) cages are similarly taken up into cells, then their role as MRI contrast agents merits further consideration. MRI probes are normally expected to clear rapidly and the large negative charge on the cages was expected to prevent their cellular uptake. Given their avid binding to serum albumin, the cages may become bound to protein to facilitate cellular uptake over a 24 hour period. Thus, the cages may not only carry the Au(I) drugs by accumulation in tumors, but they may also facilitate the uptake of the Au(I) drug into cells and influence the organelle distribution. These data suggest that future studies should focus on modification of the cage properties to modulate protein binding and to determine the effect of the modifications on cell toxicity, accumulation and animal biodistribution.

Gold-based metallacages hold significant promise for future biomedical applications, as rational design strategies[74,75] can mitigate key limitations such as poor solubility and limited targeting while enhancing delivery and biological efficacy. Continued progress in structural tuning and a deeper understanding of their interactions in complex biological environments will likely expand their scope and enable the development of more precise and multifunctional therapeutic and diagnostic platforms.[76]

Conflicts of interest

There are no conflicts to declare.

Data availability

The datasets supporting this article have been uploaded as part of the supplementary information (SI). Supplementary information: instruments and methods, synthetic procedures, NMR spectra, cell toxicity data, Schemes S1, S2, Fig. S1–S30 and Tables S1–S5. See DOI: **https://doi.org/10.1039/d6qi00661b**.

Additional data will be provided by the authors upon reasonable request.

Acknowledgements

We thank the National Institutes of Health General Medical Sciences (NIHGMS) for grant 1R16GM149396 (M. C.) and the American Cancer Society Cancer Research Institutional Grant (M. C.) DICRIDG-22-1012253-02-DICRIDG (research assistanship to F. A.). We are very grateful to the Gray Foundation (through a grant to the Brooklyn College Cancer Center) for a 2025 summer mentoring grant (A. M.). J. R. M. acknowledges the NIH (R21CA256602) for support of this research. This work utilized an ICP-MS that was purchased with funding from a NSF Major Research Instrumentation Program (NSF CHE-0959565) and National Institutes of Health (S10 RR029517 & S10 OD030397).

References

1 D. Zhang, T. K. Ronson and J. R. Nitschke, Functional capsules via subcomponent self-assembly, *Acc. Chem. Res.*, 2018, **51**, 2423–2436.
2 K. Iizuka, H. Takezawa and M. Fujita, Template and solid-state-assisted assembly of an M9L6 expanded coordination cage for medium-sized molecule encapsulation, *J. Am. Chem. Soc.*, 2024, **146**, 32311–32316.
3 J. Mosquera, T. K. Ronson and J. R. Nitschke, Subcomponent flexibility enables conversion between D 4-symmetric CdII8L8 and T-symmetric CdII4L4 assemblies, *J. Am. Chem. Soc.*, 2016, **138**, 1812–1815.
4 E. G. Percástegui, T. K. Ronson and J. R. Nitschke, Design and applications of water-soluble coordination cages, *Chem. Rev.*, 2020, **120**, 13480–13544.
5 P. R. Sahoo, J. A. Spernyak, S. G. Turowski and J. R. Morrow, Self-assembled Iron(III) coordination cage as an MRI-Active carrier for a gold(I) drug, *Bioconjugate Chem.*, 2024, **35**, 1618–1626.
6 B. Therrien, G. Süss-Fink, P. Govindaswamy, A. K. Renfrew and P. J. Dyson, The "complex–in–a–complex" cations [(acac) 2MCRu6 (p–iPrC6H4Me) 6 (tpt) 2 (dhbq) 3] 6+: a Trojan horse for cancer cells, *Angew. Chem.*, 2008, **120**, 3833–3836.
7 R. Cosialls, C. Simó, S. Borrós, V. Gómez-Vallejo, C. Schmidt, J. Llop, A. B. Cuenca and A. Casini, PET imaging of self–assembled 18F–labelled Pd2L4 metallacages for anticancer drug delivery, *Chem. – Eur. J.*, 2023, **29**, e202202604.
8 B. Woods, R. b. D. Silva, C. Schmidt, D. Wragg, M. Cavaco, V. Neves, V. F. Ferreira, L. Gano, T. n. S. Morais and F. Mendes, Bioconjugate supramolecular Pd2+metallacages penetrate the blood brain barrier in vitro and in vivo, *Bioconjugate Chem.*, 2021, **32**, 1399–1408.
9 J. Zhang, T. Pan, J. Lee, S. Goldberg, S. A. King, E. Tang, Y. Hu, L. Chen, A. Hoover and L. Zhu, Enabling tumor-specific drug delivery by targeting the Warburg effect of cancer, *Cell Rep. Med.*, 2025, **6**, 101920.
10 P. Theivendren, S. Kunjiappan, P. Pavadai, K. Ravi, A. Murugavel, A. Dayalan and A. Santhana Krishna Kumar, Revolutionizing cancer immunotherapy: emerging nanotechnology-driven drug delivery systems for enhanced therapeutic efficacy, *ACS Meas. Sci. Au*, 2024, **5**, 31–55.
11 S. Mura, J. Nicolas and P. Couvreur, Stimuli-responsive nanocarriers for drug delivery, *Nat. Mater.*, 2013, **12**, 991–1003.
12 J. Majumder and T. Minko, Multifunctional and stimuli-responsive nanocarriers for targeted therapeutic delivery, *Expert Opin. Drug Delivery*, 2021, **18**, 205–227.
13 E. Boedtkjer and S. F. Pedersen, The acidic tumor microenvironment as a driver of cancer, *Annu. Rev. Physiol.*, 2020, **82**, 103–126.
14 S.-H. Lee and J. R. Griffiths, How and why are cancers acidic? Carbonic anhydrase IX and the homeostatic control of tumour extracellular pH, *Cancers*, 2020, **12**, 1616.
15 K. E. Huntington, A. Louie, L. Zhou, A. A. Seyhan, A. W. Maxwell and W. S. El-Deiry, Colorectal cancer extracellular acidosis decreases immune cell killing and is partially ameliorated by pH-modulating agents that modify tumor cell cytokine profiles, *Am. J. Cancer Res.*, 2022, **12**, 138.
16 M. Grant, B. Cipriani, A. Corbin, D. Miller, A. Naylor, S. Hughes, T. McCarthy, S. Ambarkhane, D. Memon and M. Millward, Low pH, High Stakes: A Narrative Review Exploring the Acid-Sensing GPR65 Pathway as a Novel Approach in Renal Cell Carcinoma, *Cancers*, 2025, **17**, 3883.
17 C. Chen, D. Cai, X. Liu, Y. Zheng, X. Huang, D. Chen, J. Cai, Y. Bie, Z. Zhou and C. Hu, Lactylation of SLC26A3 in

the acidic tumor microenvironment promotes malignant progression of colorectal carcinoma, *Cell Death Dis.*, 2026, 164.

18 V. P. Torchilin, Recent advances with liposomes as pharmaceutical carriers, *Nat. Rev. Drug Discovery*, 2005, **4**, 145–160.

19 T. Yong, X. Zhang, N. Bie, H. Zhang, X. Zhang, F. Li, A. Hakeem, J. Hu, L. Gan and H. A. Santos, Tumor exosome-based nanoparticles are efficient drug carriers for chemotherapy, *Nat. Commun.*, 2019, **10**, 3838.

20 Y. Yuan, T. Nie, Y. Fang, X. You, H. Huang and J. Wu, Stimuli-responsive cyclodextrin-based supramolecular assemblies as drug carriers, *J. Mater. Chem. B*, 2022, **10**, 2077–2096.

21 Y. Yang, Q. Hu, Q. Zhang, K. Jiang, W. Lin, Y. Yang, Y. Cui and G. Qian, A large capacity cationic metal–organic framework nanocarrier for physiological pH responsive drug delivery, *Mol. Pharm.*, 2016, **13**, 2782–2786.

22 Y.-R. Zheng, K. Suntharalingam, T. C. Johnstone and S. J. Lippard, Encapsulation of Pt(IV) prodrugs within a Pt(II) cage for drug delivery, *Chem. Sci.*, 2015, **6**, 1189–1193.

23 A. Schmidt, V. Molano, M. Hollering, A. Pöthig, A. Casini and F. E. Kühn, Evaluation of new palladium cages as potential delivery systems for the anticancer drug cisplatin, *Chem. – Eur. J.*, 2016, **22**, 2253–2256.

24 I. A. Bhat, R. Jain, M. M. Siddiqui, D. K. Saini and P. S. Mukherjee, Water-soluble Pd8L4 self-assembled molecular barrel as an aqueous carrier for hydrophobic curcumin, *Inorg. Chem.*, 2017, **56**, 5352–5360.

25 Z. Yue, H. Wang, D. J. Bowers, M. Gao, M. Stilgenbauer, F. Nielsen, J. T. Shelley and Y.-R. Zheng, Nanoparticles of metal–organic cages designed to encapsulate platinum-based anticancer agents, *Dalton Trans.*, 2018, **47**, 670–674.

26 G. Moreno-Alcántar, M. Drexler and A. Casini, Assembling a new generation of radiopharmaceuticals with supramolecular theranostics, *Nat. Rev. Chem.*, 2024, **8**, 893–914.

27 W.-T. Dou, C.-Y. Yang, L.-R. Hu, B. Song, T. Jin, P.-P. Jia, X. Ji, F. Zheng, H.-B. Yang and L. Xu, Metallacages and covalent cages for biological imaging and therapeutics, *ACS Mater. Lett.*, 2023, **5**, 1061–1082.

28 B. P. Burke, W. Grantham, M. J. Burke, G. S. Nichol, D. Roberts, I. Renard, R. Hargreaves, C. Cawthorne, S. J. Archibald and P. J. Lusby, Visualizing kinetically robust CoIII4L6 assemblies in vivo: SPECT imaging of the encapsulated [99mTc] TcO4−anion, *J. Am. Chem. Soc.*, 2018, **140**, 16877–16881.

29 R. Wang, L. An, J. He, M. Li, J. Jiao and S. Yang, A class of water-soluble Fe(III) coordination complexes as T 1-weighted MRI contrast agents, *J. Mater. Chem. B*, 2021, **9**, 1787–1791.

30 Y.-X. Chen, M.-S. Qiu, J.-S. Hu, H.-L. Yue, M. Yu, S.-Z. Chen, X. Zhou and J. Tao, Insights into host-guest interactions and enhanced MRI contrast applications of water-soluble tetrahedral metal-organic cages, *Sci. China: Chem.*, 2025, **68**, 3536–3545.

31 G. E. Sokolow, M. R. Crawley, D. R. Morphet, D. Asik, J. A. Spernyak, A. R. McGray, T. R. Cook and J. R. Morrow, Metal– organic polyhedron with four Fe(III) centers producing enhanced T1 magnetic resonance imaging contrast in tumors, *Inorg. Chem.*, 2022, **61**, 2603–2611.

32 G. Moreno-Alcántar, P. Picchetti and A. Casini, Gold complexes in anticancer therapy: from new design principles to particle–based delivery systems, *Angew. Chem., Int. Ed.*, 2023, **62**, e202218000.

33 Y. Lu, X. Ma, X. Chang, Z. Liang, L. Lv, M. Shan, Q. Lu, Z. Wen, R. Gust and W. Liu, Recent development of gold(I) and gold(III) complexes as therapeutic agents for cancer diseases, *Chem. Soc. Rev.*, 2022, **51**, 5518–5556.

34 M. R. Chang, E. M. Matnurov, C. Wu, J. Arakelyan, H.-J. Choe, V. Kushnarev, J. Y. Yap, X. X. Soo, M. J. Chow, W. Berger, W. H. Ang and M. V. Babak, Leveraging Immunogenic Cell Death to Enhance the Immune Response against Malignant Pleural Mesothelioma Tumors, *J. Am. Chem. Soc.*, 2025, **147**, 7908–7920.

35 F. H. Abdalbari and C. M. Telleria, The gold complex auranofin: new perspectives for cancer therapy, *Discover Oncol.*, 2021, **12**, 42.

36 A. Ahad, F. Aftab, A. Michel, J. S. Lewis and M. Contel, Development of immunoliposomes containing cytotoxic gold payloads against HER2-positive breast cancers, *RSC Med. Chem.*, 2024, **15**, 139–150.

37 Y. Marciano, N. Nayeem, D. Dave, R. V. Ulijn and M. Contel, N-acetylation of biodegradable supramolecular peptide nanofilaments selectively enhances their proteolytic stability for targeted delivery of gold-based anticancer agents, *ACS Biomater. Sci. Eng.*, 2023, **9**, 3379–3389.

38 Y. Marciano, V. Del Solar, N. Nayeem, D. Dave, J. Son, M. Contel and R. V. Ulijn, Encapsulation of gold-based anticancer agents in protease-degradable peptide nanofilaments enhances their potency, *J. Am. Chem. Soc.*, 2022, **145**, 234–246.

39 D. L. Caulder, C. Brückner, R. E. Powers, S. König, T. N. Parac, J. A. Leary and K. N. Raymond, Design, formation and properties of tetrahedral M4L4 and M4L6 supramolecular clusters1, *J. Am. Chem. Soc.*, 2001, **123**, 8923–8938.

40 Z. J. Wang, C. J. Brown, R. G. Bergman, K. N. Raymond and F. D. Toste, Hydroalkoxylation catalyzed by a gold(I) complex encapsulated in a supramolecular host, *J. Am. Chem. Soc.*, 2011, **133**, 7358–7360.

41 D. M. Kaphan, M. D. Levin, R. G. Bergman, K. N. Raymond and F. D. Toste, A supramolecular microenvironment strategy for transition metal catalysis, *Science*, 2015, **350**, 1235–1238.

42 A. Dissanayake, J. A. Spernyak and J. R. Morrow, An octahedral coordination cage with six Fe (iii) centers as a T 1 MRI probe, *Chem. Commun.*, 2024, **60**, 12249–12252.

43 J. E. López-Hernández and M. Contel, Promising heterometallic compounds as anticancer agents: Recent studies in vivo, *Curr. Opin. Chem. Biol.*, 2023, **72**, 102250.

44 B. T. Elie, J. Fernández-Gallardo, N. Curado, M. A. Cornejo, J. W. Ramos and M. Contel, Bimetallic titanocene-gold phosphane complexes inhibit invasion, metastasis, and

angiogenesis-associated signaling molecules in renal cancer, *Eur. J. Med. Chem.*, 2019, **161**, 310–322.

45 A. Ahad, H. K. Saeed, V. Del Solar, J. E. López-Hernández, A. Michel, J. Mathew, J. S. Lewis and M. Contel, Shifting the antibody–drug conjugate paradigm: a trastuzumab-gold-based conjugate demonstrates high efficacy against human epidermal growth factor receptor 2-positive breast cancer mouse model, *ACS Pharmacol. Transl. Sci.*, 2023, **6**, 1972–1986.

46 M. D. Pluth, R. G. Bergman and K. N. Raymond, Proton-mediated chemistry and catalysis in a self-assembled supramolecular host, *Acc. Chem. Res.*, 2009, **42**, 1650–1659.

47 M. D. Pluth, R. G. Bergman and K. N. Raymond, Acid catalysis in basic solution: a supramolecular host promotes orthoformate hydrolysis, *Science*, 2007, **316**, 85–88.

48 J. S. Mugridge, G. Szigethy, R. G. Bergman and K. N. Raymond, Encapsulated guest– host dynamics: guest rotational barriers and tumbling as a probe of host interior cavity space, *J. Am. Chem. Soc.*, 2010, **132**, 16256–16264.

49 T. K. Piskorz, V. Martí-Centelles, R. L. Spicer, F. Duarte and P. J. Lusby, Picking the lock of coordination cage catalysis, *Chem. Sci.*, 2023, **14**, 11300–11331.

50 Q. Chen, M. G. Espey, A. Y. Sun, J.-H. Lee, M. C. Krishna, E. Shacter, P. L. Choyke, C. Pooput, K. L. Kirk and G. R. Buettner, Ascorbate in pharmacologic concentrations selectively generates ascorbate radical and hydrogen peroxide in extracellular fluid in vivo, *Proc. Natl. Acad. Sci. U. S. A.*, 2007, **104**, 8749–8754.

51 N. G. Baranska, A. Parkin and A.-K. Duhme-Klair, Electrochemical and solution structural characterization of Fe(III) azotochelin complexes: examining the coordination behavior of a tetradentate siderophore, *Inorg. Chem.*, 2022, **61**, 19172–19182.

52 L. Galluzzi, E. Guilbaud, D. Schmidt, G. Kroemer and F. M. Marincola, Targeting immunogenic cell stress and death for cancer therapy, *Nat. Rev. Drug Discovery*, 2024, **23**, 445–460.

53 L. Galluzzi, O. Kepp, E. Hett, G. Kroemer and F. M. Marincola, Immunogenic cell death in cancer: concept and therapeutic implications, *J. Transl. Med.*, 2023, **21**, 162.

54 J. X. Zou, M. R. Chang, N. A. Kuznetsov, J. X. Kee, M. V. Babak and W. H. Ang, Metal-based immunogenic cell death inducers for cancer immunotherapy, *Chem. Sci.*, 2025, **16**, 6160–6187.

55 S. V. Hato, A. Khong, I. J. M. de Vries and W. J. Lesterhuis, Molecular pathways: the immunogenic effects of platinum-based chemotherapeutics, *Clin. Cancer Res.*, 2014, **20**, 2831–2837.

56 E. Catanzaro, M. Beltrán-Visiedo, L. Galluzzi and D. V. Krysko, Immunogenicity of cell death and cancer immunotherapy with immune checkpoint inhibitors, *Cell. Mol. Immunol.*, 2025, **22**, 24–39.

57 S. Sen, S. Hufnagel, E. Y. Maier, I. Aguilar, J. Selvakumar, J. E. DeVore, V. M. Lynch, K. Arumugam, Z. Cui and J. L. Sessler, Rationally designed redox-active Au(I) N-heterocyclic carbene: an immunogenic cell death inducer, *J. Am. Chem. Soc.*, 2020, **142**, 20536–20541.

58 H. Van Le, M. V. Babak, M. A. Ehsan, M. Altaf, L. Reichert, A. L. Gushchin, W. H. Ang and A. A. Isab, Highly cytotoxic gold(I)-phosphane dithiocarbamate complexes trigger an ER stress-dependent immune response in ovarian cancer cells, *Dalton Trans.*, 2020, **49**, 7355–7363.

59 R. D. Mule, A. Kumar, S. P. Sancheti, B. Senthilkumar, H. Kumar and N. T. Patil, BQ-AurIPr: a redox-active anti-cancer Au (i) complex that induces immunogenic cell death, *Chem. Sci.*, 2022, **13**, 10779–10785.

60 Z. Yang, M. Bian, L. Lv, X. Chang, Z. Wen, F. Li, Y. Lu and W. Liu, Tumor-targeting NHC–Au(I) complex induces immunogenic cell death in hepatocellular carcinoma, *J. Med. Chem.*, 2023, **66**, 3934–3952.

61 Z. Xu, Q. Lu, M. Shan, G. Jiang, Y. Liu, Z. Yang, Y. Lu and W. Liu, NSAID–Au(I) complexes induce ROS-driven DAMPs and interpose inflammation to stimulate the immune response against ovarian cancer, *J. Med. Chem.*, 2023, **66**, 7813–7833.

62 Y. Lu, X. Sheng, C. Liu, Z. Liang, X. Wang, L. Liu, Z. Wen, Z. Yang, Q. Du and W. Liu, SERD-NHC-Au(I) complexes for dual targeting ER and TrxR to induce ICD in breast cancer, *Pharmacol. Res.*, 2023, **190**, 106731.

63 F. Li, Z. Wen, C. Wu, Z. Yang, Z. Wang, W. Diao, D. Chen, Z. Xu, Y. Lu and W. Liu, Simultaneous activation of immunogenic cell death and cGAS-STING pathway by liver-and mitochondria-targeted gold(I) complexes for chemoimmunotherapy of hepatocellular carcinoma, *J. Med. Chem.*, 2024, **67**, 1982–2003.

64 W.-J. Li, S.-H. Li, X.-Y. Man, G. Xu, Z.-L. Zhang, Y. Zhang, H. Liang and F. Yang, A novel Au(III) agent designed to inhibit tumor growth and metastasis through inducing immunogenic cell death, *Rare Met.*, 2025, **44**, 430–443.

65 T. Babu, M. S. Levine, S. Acharya, E. Y. Maier and J. L. Sessler, Three is better than one: a multimetal complex that triggers immunogenic cell death, *Angew. Chem.*, 2025, **137**, e202514351.

66 J. Zhou, G. Wang, Y. Chen, H. Wang, Y. Hua and Z. Cai, Immunogenic cell death in cancer therapy: Present and emerging inducers, *J. Cell. Mol. Med.*, 2019, **23**, 4854–4865.

67 K.-C. Mei, Y.-P. Liao, J. Jiang, M. Chiang, M. Khazaieli, X. Liu, X. Wang, Q. Liu, C. H. Chang and X. Zhang, Liposomal delivery of mitoxantrone and a cholesteryl indoximod prodrug provides effective chemo-immunotherapy in multiple solid tumors, *ACS Nano*, 2020, **14**, 13343–13366.

68 V. Vukovic and I. Tannock, Influence of low pH on cytotoxicity of paclitaxel, mitoxantrone and topotecan, *Br. J. Cancer*, 1997, **75**, 1167–1172.

69 M. Enache and E. Volanschi, Spectral characterization of self-association of antitumor drug mitoxantrone, *Rev. Roum. Chim.*, 2010, **55**, 255–262.

70 T. Panaretakis, O. Kepp, U. Brockmeier, A. Tesniere, A.-C. Bjorklund, D. C. Chapman, M. Durchschlag, N. Joza, G. Pierron and P. Van Endert, Mechanisms of pre-apoptotic

calreticulin exposure in immunogenic cell death, *EMBO J.*, 2009, **28**, 578.

71 A. Nyga, K. Plak, M. Kräter, M. Urbanska, K. Kim, J. Guck and B. Baum, Dynamics of cell rounding during detachment, *Iscience*, 2023, **26**, 106696.

72 J. Mitchell and K. W.-H. Lo, The use of small-molecule compounds for cell adhesion and migration in regenerative medicine, *Biomedicines*, 2023, **11**, 2507.

73 R. W. Putnam, Chapter 17 - Intracellular pH regulation, in *Cell Physiology Source Book*, ed. N. Sperelakis, Academic Press, 4th edn, 2012, pp. 303–321.

74 N. Willnhammer, F. A. Böhm, C. Vlaswinkel, L. Rieder, D. Bogenberger, D. Krauss, J. Zuber, B. van der Wildt, A. Poot and A. Pöthig, Post-assembly modification of Pt(II) metallacages provides an open door to medicinal applications, *Cell Rep. Phys. Sci.*, 2026, 103249.

75 M. Drexler, I. Kanavos, D. Krauss, G. Moreno-Alcántar, L. M. Smith, M. E. George, T. H. Witney, R. Lobinski, L. Ronga and A. Casini, Design of porous self-assembled homoleptic and heteroleptic Pd 2+cages incorporating silicon-based fluoride acceptors: the way towards nuclear imaging applications, *Inorg. Chem. Front.*, 2025, **12**, 6309–6325.

76 S. R. Thomas, N. Willnhammer, A. Casini and G. Moreno-Alcántar, Gold metallacages: Design principles and applications, *Chem*, 2025, **11**, 102502.

